PALEONTOLOGY

Highly aquatic marine stem archosaur with soft tissue preservation

Wei Wang[1]*, Nicholas C. Fraser[2], Stephan N. F. Spiekman[3,4], Zhiheng Li[1], Olivier Rieppel[5], Hong Lei[6], Torsten M. Scheyer[7], Chun Li[1]*

Archosauromorpha is a dominant reptile clade that primarily occupied terrestrial ecosystems with limited secondarily aquatic invasions that are poorly known. Here we report on a well-preserved Triassic reptile representing the earliest stem-archosaur to evolve unequivocal aquatic specializations. This taxon exhibits a suite of aquatic adaptations previously unknown in stem-archosaurs, such as hyperphalangy, enhanced paddle-like forelimbs, and a loss of articulation between the sacrum and pelvis, indicating an advanced aquatic lifestyle. The fossil exhibits the oldest known stomach, liver, and intestinal preservations in reptiles. Our findings provide unexpected insights into the early aquatic diversification of Archosauromorpha during the Triassic marine ecosystem recovery and highlight a conservative gastrointestinal system in an early Mesozoic vertebrate. In the absence of clear terrestrial members of the other major Mesozoic marine reptile lineages (e.g., ichthyosaurs and sauropterygians), this discovery provides an unambiguous example of such a lineage including both decidedly terrestrial and extensively marine forms, providing tantalizing evidence for the land-to-sea transition in Triassic reptiles.

INTRODUCTION

The end-Permian mass extinction event triggered major subsequent ecological reorganizations, with multiple reptilian lineages colonizing marine environments during the Triassic (*1*), among which sauropterygians (*2*) and ichthyosaurs (*3*, *4*) emerged as quintessential marine predators throughout Mesozoic times. Concurrently, archosauromorphs, the clade including crown-group archosaurs and their stem relatives, rose to dominate terrestrial ecosystems for more than 180 million years (*5*–*7*). This broad terrestrial-marine ecological dichotomy has long framed our understanding of reptilian evolution (*1*), with marine archosauromorphs being relatively rare and less well studied (*8*). Within crown-group archosaurs besides sea birds, crocodylians are known to include many aquatic forms and a few non-avian dinosaurs have been postulated to have been semiaquatic or subaqueous foragers (*9*–*11*). The crocodile-line Thalattosuchia represent the most diverse and extensively adapted aquatic lineage within archosaurs (*12*), including obligatorily marine members from the Middle Jurassic to the Early Cretaceous (*13*). During the Triassic, phytosaurs (*14*) and some other archosauriforms (e.g., *Qianosuchus mixtus*, *Litorosuchus somnii*, and *Vancleavea campi*) (*15*–*17*) also occur in freshwater or marine sediments and exhibit features of a semiaquatic lifestyle.

Tanysauria (*18*) represents one of the earliest diverging clades of archosauromorphs with fossil remains from the Early Triassic (*6*, *19*, *20*). Many of these long-necked archosauromorphs were almost certainly terrestrial, such as *Macrocnemus* and *Pectodens* (*21*, *22*). However, the two recognized tanysaurian families, Tanystropheidae and Trachelosauridae, also include semiaquatic to marine taxa, which both exhibit independently attained adaptations for an aquatic lifestyle, including extreme neck elongation, as is most clearly expressed in the tanystropheid *Tanystropheus* and the trachelosaurid *Dinocephalosaurus* (*23*–*25*). The trachelosaurids, in particular, represent the archosauromorphs most extensively adapted for marine life, potentially rivaling contemporaneous sauropterygians and ichthyosaurs in this regard. In the emblematic *Dinocephalosaurus*, these adaptations include an elongate snake-like body (*2*) and paddle-like limbs (*25*). Despite having only recently been recognized as a distinct clade (*19*), recent fossil discoveries and revisions of historical material alike provide a tantalizing indication of the diversity of marine trachelosaurids in Middle Triassic oceans (*18*, *26*, *27*). However, aside from *Dinocephalosaurus*, this evidence has been restricted to isolated elements or partial skeletons lacking articulated appendicular remains. Consequently, the morphological disparity and locomotory strategies of tanysaurs, and how they compare to other marine amniote lineages, remains poorly understood.

In this study, we describe a complete skeleton of *Austronaga minuta*, a recently erected tanysaur from southwestern China (*27*). This exceptional specimen preserves not only a complete skeleton but also rare soft tissue remains within the body cavity, providing unprecedented insights into both the osteological and visceral anatomy of early archosauromorphs. This animal displays highly specialized limbs adapted for subaqueous locomotion, an observation supported by our analyses of a large sample of secondarily aquatic amniotes. This discovery provides definitive evidence of an obligate aquatic early stem archosaur, revealing a previously unrecognized marine ecological niche in Archosauromorpha.

[1]Institute of Vertebrate Paleontology and Paleoanthropology, Chinese Academy of Sciences, Beijing 100044, China. [2]National Museums Scotland, Chambers Street, Edinburgh EH1 1 JF, UK. [3]Staatliches Museum für Naturkunde Stuttgart, Rosenstein 1, 10191 Stuttgart, Germany. [4]University of Hohenheim, Department of Paleontology, Institute of Biology, 70599 Stuttgart, Germany. [5]Department of Geology, The Field Museum, 1400 S. Lake Shore Drive, Chicago, IL 60605, USA. [6]Luoping Biota National Geopark, Land and Resources Bureau of Luoping County, Yunnan 655800, China. [7]University of Zurich, Department of Paleontology, Karl Schmid-Strasse 4, 8006 Zurich, Switzerland.
*Corresponding author. Email: wangwei2014@ivpp.ac.cn (W.W.); lichun@ivpp.ac.cn (C.L.)

RESULTS

Systematic paleontology

Diapsida, Osborn, 1903.
Archosauromorpha, von Huene, 1946.
Tanysauria, Spiekman *et al.*, 2024.
Trachelosauridae, Abel 1919 (sensu Spiekman *et al.*, 2024).
Austronaga minuta, Wang *et al.*, 2023.

Type specimen

Institute of Vertebrate Paleontology and Paleoanthropology (IVPP) V18579, a complete articulated skeleton preserved on two slabs (Fig. 1).

Locality and horizon

Waina Village, Luoping County, Yunnan Province, China; Member II of Guanling Formation, middle Anisian (Pelsonian), Middle Triassic.

Emended diagnosis

A tanysaur with the following features: quadrate anteroposteriorly broad and plate-like in lateral view with concave posterior margin; 18 cervical, 24 dorsal vertebrae; tall axe-shaped neural spine on axis; cervical neural spines prominent, with convex dorsal margin and without anterodorsal or posterodorsal projections; chevrons of mid-caudal region hatchet-shaped, with prominent distal expansion and a notch at the midpoint of its ventral margin; forelimb distinctly longer than hindlimb with humerus to femur length ratio over two; hyperphalangy present in both manus and pes.

Description

Skeletal anatomy

The skeleton is exceptionally well preserved on two slabs (Figs. 1 and 2) and partially described in a previous report (*27*). The entire vertebral column comprises 18 cervical, 24 dorsal, two sacral, and 71 caudal vertebrae. This highlights the high variability in presacral vertebral counts observed in trachelosaurids, considering that *Dinocephalosaurus* and *Trachelosaurus* have 32 cervical and 30 dorsal vertebrae and approximately 21 cervical and 27 dorsal vertebrae, respectively (*18*, *25*). This stands in stark contrast with the much more conservative presacral vertebral counts of the trachelosaurid sister clade Tanystropheidae

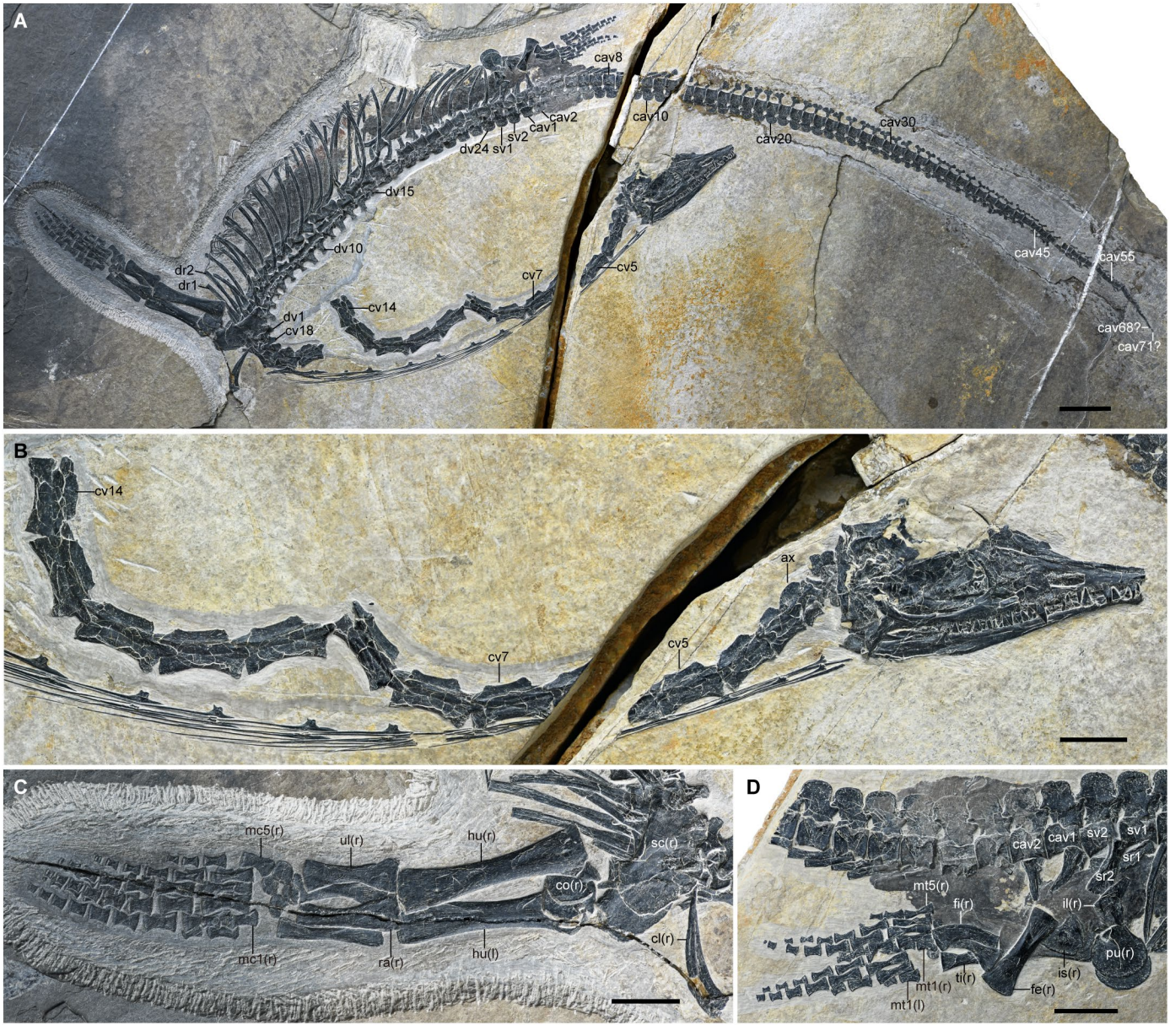

Fig. 1. Skeleton of the holotype of *Austronaga minuta* (IVPP V18579). Abbreviations are in the Supplementary Materials. Scale bars, 2 cm (**A**) and 1 cm (**B** to **D**).

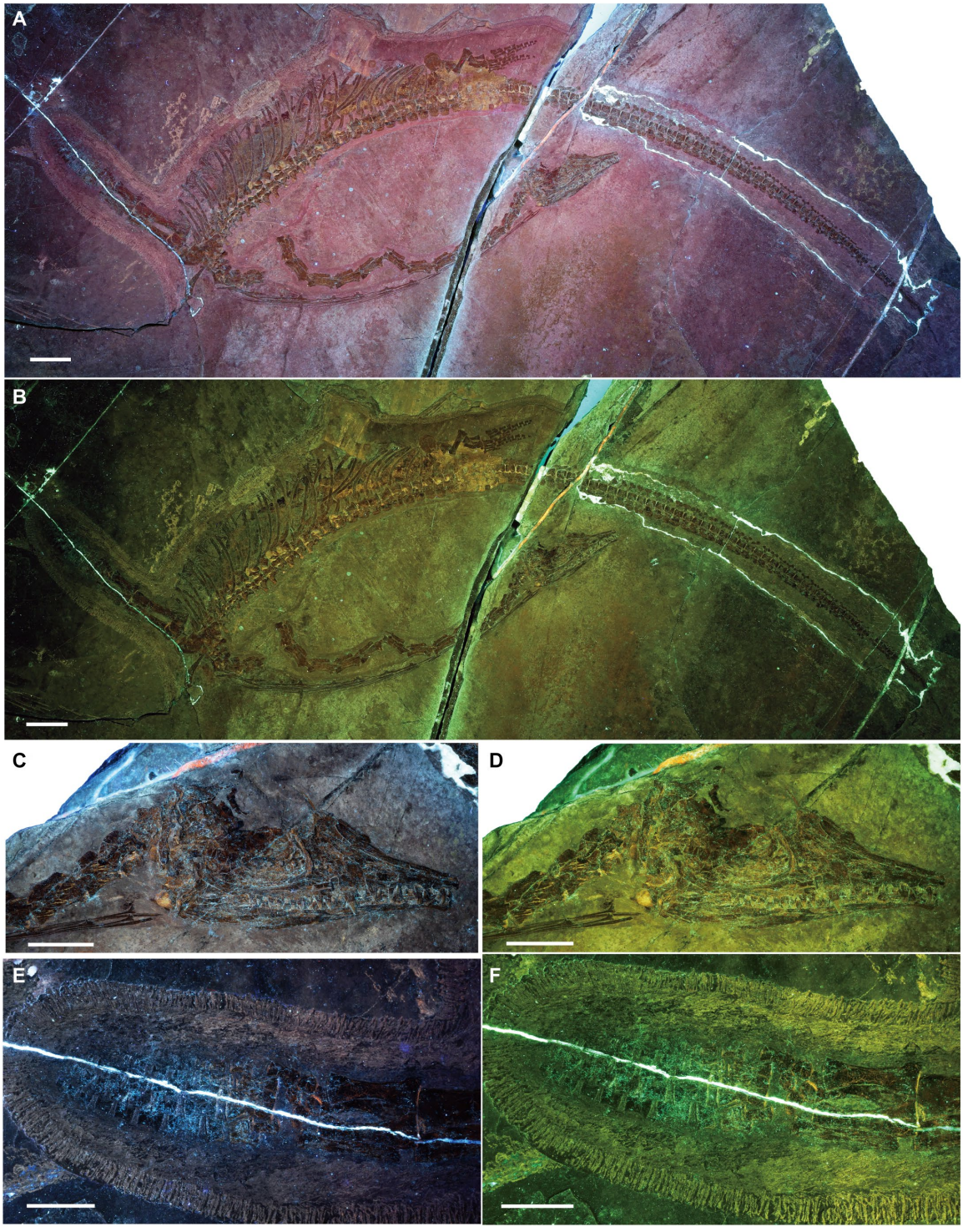

Fig. 2. IVPP V18579 under UV light. (**A** and **B**) skeleton under UV without and with yellow filter. Scale bar, 2 cm. (**C** and **D**) Skull under UV without and with yellow filter. Scale bar, 1 cm. (**E** and **F**) Manus under UV without and with yellow filter. Scale bar, 1 cm.

(*28*). Apart from the most anterior and posterior cervical vertebrae, the dorsal margin of the cervical neural spine is slightly concave in lateral view and reminiscent of the trachelosaurids *Pectodens* (*22*) and *Dinocephalosaurus* (*25*). Absence of anterior and posterior expansions of the neural spine in lateral view, as well as the absence of a transverse expansion of their distal margin in *Austronaga*, also provides added resemblance to *Dinocephalosaurus* and *Pectodens*. In the anterior to middle dorsal vertebrae, the transverse processes display a distinct vertical ventral ridge (fig. S3), reminiscent of the condition observed in *Dinocephalosaurus*, *Pectodens*, and *Trachelosaurus* (*18*, *22*, *25*), likely representing a trachelosaurid synapomorphy. The distal expansion of the sacral rib is reduced and not as broad or bifurcate as in other tanysaurians (*19*, *21*), resulting in a loose articulation with the pelvic elements.

The scapula is characterized by a relatively tall and broad semicircular dorsal blade, which contrasts with the relatively low, kidney-shaped bone observed in *Tanystropheus*, *Macrocnemus*, and *Fuyuansaurus* (*29*–*32*), but more closely resembles that of *Dinocephalosaurus* (*25*). Notably, the scapula is distinctly larger than the coracoid in *Austronaga*, a feature not previously observed in any tanysaur (Fig. 1 and fig. S5). The coracoid exhibits a notched anterior margin located below the glenoid, and no coracoid foramen is exposed, but it might conceivably be covered by overlying elements in both coracoids. The paired clavicles are quite long, robust, and slightly curved elements that taper gently toward what would have constituted a dorsal contact with the scapula. There is no indication of an ossified interclavicle. The humeri are fairly straight and elongate, pillar-like elements with both slightly concave pre- and postaxial margins. There are no pronounced condyles or trochleae developed on the ends of the humeri, radii, or ulnae. Only two disc-shaped carpals are ossified, and the articulation between the carpals and the metacarpals is weak with a large gap between them (Fig. 1 and fig. S5). The metacarpals in *Austronaga* are relatively short, with the ratio between the lengths of the metacarpal and the most proximal phalanx in the same digit less than 1.5, which is similar to that of *Dinocephalosaurus* but lower than in other known tanysaurs that lack flippered limbs (e.g., *Pectodens*, *Macrocnemus*, and *Tanystropheus*) (*22*, *29*, *32*). We obtain the preserved phalangeal formula for the fully exposed right manus as 1:7:6:5:3, in sharp contrast to 2:3:4:5:3 (or 4) in *Pectodens* (*22*) and 2:3:4:5:3 in *Protorosaurus* (*33*). The manus in *Austronaga* shows an exceptional case of hyperphalangy in the middle digits (Fig. 1 and fig. S5) also compared with *Dinocephalosaurus*, which conversely exhibits a phalangeal reduction relative to other tanysaurians (*25*). Although hyperphalangy is common in other highly marine reptile clades (e.g., Plesiosauria and Ichthyopterygia), it has not previously been identified among Archosauromorpha. Akin to the specimens of *Dinocephalosaurus* (*25*, *27*, *34*), we note that most of the preserved distal phalanges, like many other tetrapods with well-developed flippers, do not exhibit the typical "clawed" morphology of an ungual but are poorly ossified as rectangular thin pieces of bone evidently smaller than other phalanges and possibly with cartilaginous distal ends.

The ilium is a small element that lacks a preacetabular process and which has a dorsally oriented postacetabular process. This differs distinctly from the posteriorly or posterodorsally oriented postacetabular process of other archosauromorphs (*6*). This iliac configuration provides further indication of a severely limited contact with the sacral ribs. The morphology of the pubis and ischium resembles that of *Dinocephalosaurus* and is distinct from other tanysaurs (*25*). The configuration of the pelvic elements also differs from other known Triassic archosauromorphs (*6*) by having a pubis that is considerably larger than the ischium (Fig. 1 and fig. S4). This pelvic morphology in *Austronaga* is reminiscent of that in sauropterygians or sauropterygiforms such as *Hanosaurus* in showing a reduced iliac blade and a subcircular pubis larger than the kidney-shaped ischium (*2*). Compared to the forelimb, the hindlimb is evidently much reduced in size. The femur is pillar-shaped, developing weakly concave preaxial and postaxial margins and equally expanded at both ends, similar to the femora of *Dinocephalosaurus* and *Trachelosaurus* (*18*, *25*). Only one ossified tarsal can be identified in *Austronaga*. As for the forelimb, all the articular surfaces on the bony elements in this hindlimb are vestigial. The phalangeal formula for the pes is 1:2:6:5:3 based on the right side, with the count on the left pes being partially obscured but broadly similar. There is a degree of hyperphalangy in the middle digits when compared with *Dinocephalosaurus* (*25*) and other Triassic archosauromorphs (*6*). Overall, the hindlimbs of *Austronaga* are the most poorly developed of all hitherto known early archosauromorphs (*6*).

Soft tissue anatomy

The most anterior part of soft tissue represents the stomach on the basis of its relative position, size, and shape (Figs. 2 and 3 and figs. S6 to S8). Some fiber-like branching structures can also be observed (Fig. 4), which might represent capillary-sized blood vessels (*35*). Posteroventrally to the stomach, there is a remarkably thin layer with a reddish hue, extending from the distal portions of the 9th to 14th dorsal vertebrae (Fig. 3 and fig. S6). On the basis of its position and distinctive color, this second mass represents the liver (*35*, *36*). This interpretation is supported by the fact that the liver is comparatively rich in iron, and the reddish matter is likely due to deposition of hematite that appears dark black under ultraviolet (UV) light (Figs. 2 and 3 and fig. S6). A layer of framboidal ferriferous material is detected in this part with a distinctly high iron component (Fig. 5). Within the abdominal cavity situated between the 17th dorsal and the 1st sacral vertebra, there are dark brown cololites with smooth surfaces. The anterior portion of this mass is arranged in loops that are relatively narrow compared to the posterior section (Figs. 2 and 3), and it is suggested that these remains represent the small intestine and the large colon. The posterior part is darker and thicker and encrusts the 22nd to 25th dorsal vertebrae and ribs and exhibits a three-dimensional structure. It contains pieces of undigested food, possibly including ganoid fish scales (Fig. 3 and fig. S7). A remarkably high concentration of phosphates is present in this region compared with other areas (Figs. 6 and 7 and figs. S12 to S14). Posterior to the sacrum, the most posterior mass of soft tissue appears as a light brownish mass around the presumed position of the vent and extends dorsally to cover the anterior five caudal vertebrae (Figs. 2 and 3 and fig. S8). This is tentatively considered to be skin and muscle remains, although it lacks the discernible scales described in other tanysaurs with such preservation (*37*, *38*), but the scales are commonly vestigial in highly aquatic reptiles.

DISCUSSION

The skeleton of *Austronaga* was recovered from marine sediments in Luoping, China, where it occurs together with abundant marine invertebrates, fishes, and other marine reptiles in the eastern Tethys (*39*). An array of anatomical features collectively demonstrates its extensive aquatic adaptations. The narial position, located posteriorly rather than at the rostral tip, likely aided in surface respiration (*40*). The jaws have conical teeth with prominent fangs, a dental morphology

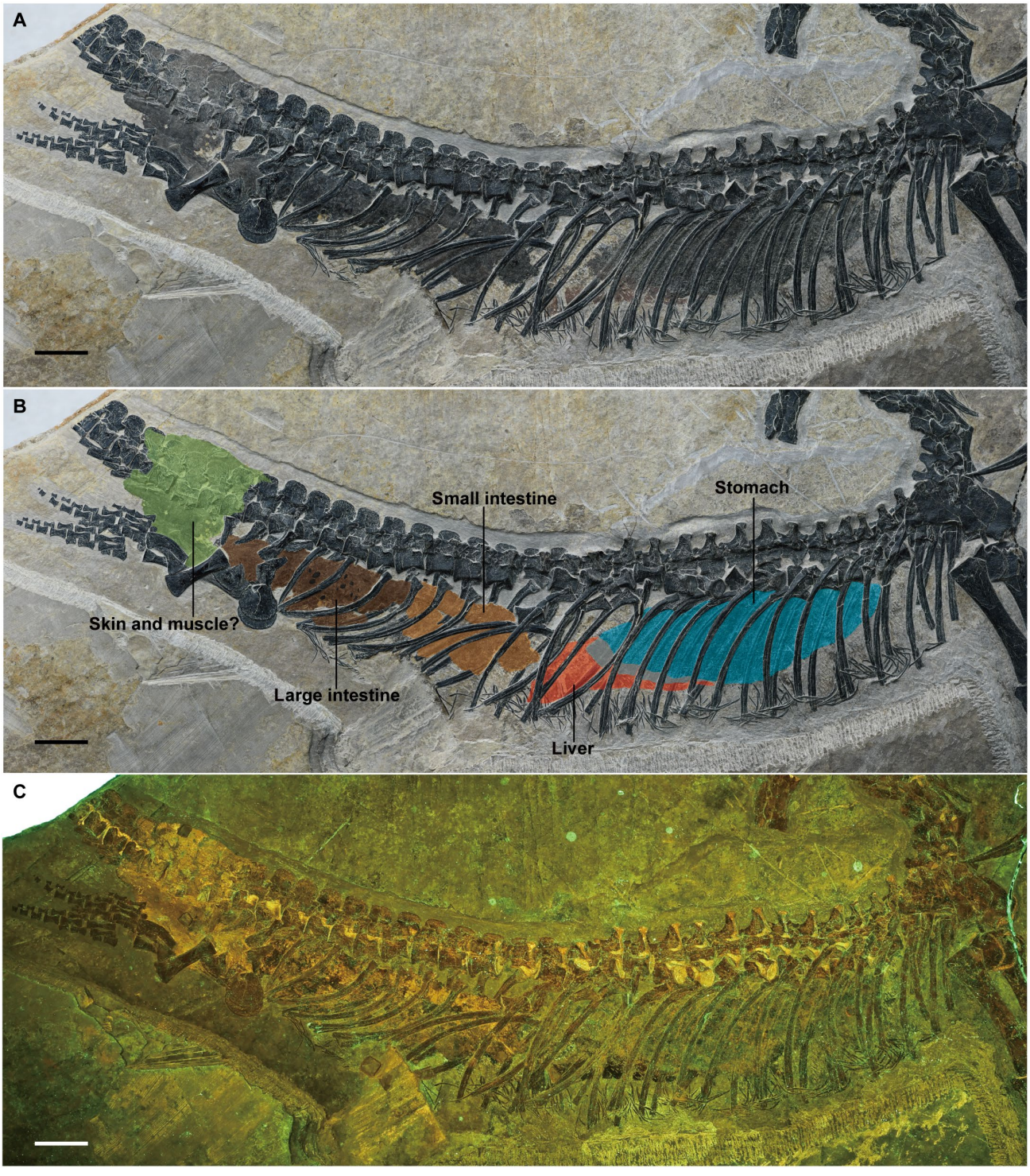

Fig. 3. Gastrointestinal preservation in IVPP V18579. (**A**) Under normal light; (**B**) interpretation; (**C**) under UV light with yellow filter; scale bar, 1 cm.

characteristic of piscivorous reptiles (*41*). This interpretation is further supported by the fish scales preserved as stomach contents, suggesting that *Austronaga* actively preyed on small fishes (Fig. 3 and fig. S7). The scapula, coracoid, pubis, and ischium are thin and plate-like resembling other marine reptiles (*2*, *3*). By contrast, in terrestrial relatives, these elements have irregular outlines with discrete blades and thickened margins (*15*, *32*). Notably in *Austronaga*, the pelvic girdle is substantially reduced with the loss of articulation between the sacral ribs and the heavily modified ilium, indicating minimal weight-bearing capacity for terrestrial locomotion (*42*). By contrast, the pelvic girdles of the semiaquatic taxa such as *Litorosuchus* and *Vancleavea* are relatively more reinforced (*16*, *17*).

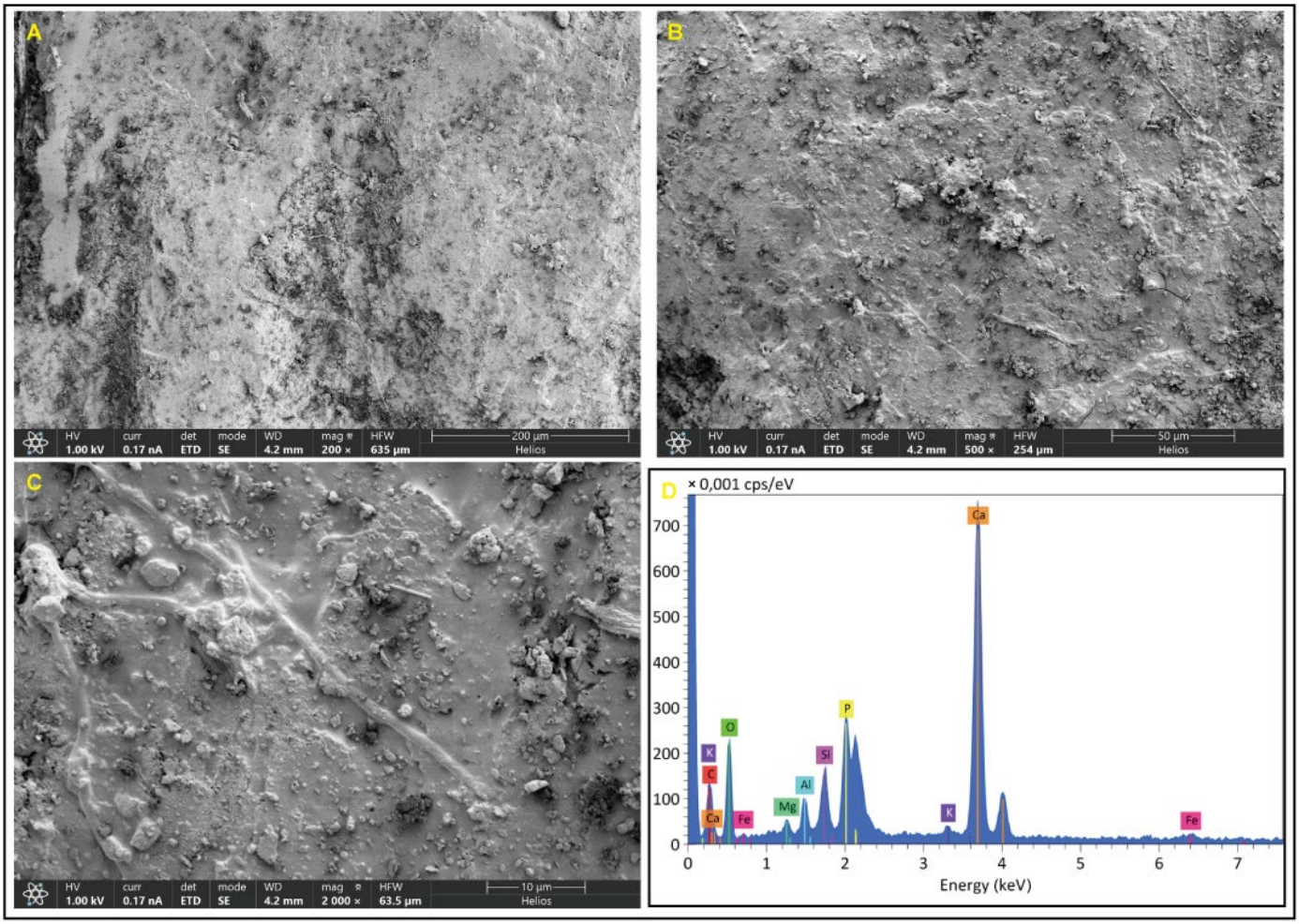

Fig. 4. Microstructure and element contents from the stomach under SEM. This is sample 2 shown in fig. S9 located at the anterior part of the stomach; (**A** to **C**) are the SEM images under different scales; (**D**) is the elemental analysis obtained from the region in (A).

The most specialized aquatic adaptations in *Austronaga* are evident in its limb morphology (Fig. 8 and figs. S4 and S5). Two previous studies have independently proposed quantitative frameworks linking limb proportions to the degree of aquatic adaptation: one focused on humerus and femur lengths (*43*), while the other investigated full limb proportions (*44*). On the basis of the previous data and additionally included measurements in this study (see Materials and Methods for more details), our comparative analyses of limb proportions across extinct and extant secondarily aquatic reptiles and mammals (data S1 and S2, Fig. 9, and figs. S17 to S26) demonstrate that *Austronaga* is an obligate aquatic animal exhibiting more pronounced marine adaptations than most secondarily aquatic non-avian amniotes (avians are not included in the analysis because of their aberrant forelimb morphology due to the typical bird wing). A femur shorter than the humerus represents a robust indicator of an advanced stage of aquatic adaptation (*43*, *44*). In aquatic amniotes, the support from the hindlimb is redundant and the center of mass shifted anteriorly near the buoyancy center, optimizing submerged balance. The ratio between the lengths of the humerus and femur in *Austronaga* is 2.19. It is the highest value among all marine tetrapods (figs. S16 and S19) sampled in our two datasets (183 samples in data S1 and 230 samples in data S2) and compares directly to a previous review of secondarily aquatic adaptation in vertebrates (*43*). *Austronaga* also has the highest value of the ratio in both datasets when the lengths of the humerus and femur are $\log_{10}$-transformed (Fig. 9A and figs. S17, S18, and S20) and shows a forelimb much longer than the hindlimb (Fig. 8) in comparison with other aquatic amniotes (figs. S21 to S23). Beyond limb length ratios, elongated autopodia (manus and pes) (Fig. 9B and figs. S24 to S26) exhibiting hyperphalangy (i.e., supranumeral phalanges in at least one digit) is another significant indicator of aquatic specialization, as demonstrated in certain amniote groups (e.g., plesiosaurs, ichthyosaurs, mosasaurs, pinnipeds, and cetaceans) (*44*–*47*). These elongate forelimbs and large autopodia with hyperphalangy are absent in semiaquatic Triassic archosauriforms like *Litorosuchus* and *Vancleavea* (*16*, *17*). *Austronaga* and *Dinocephalosaurus* display large autopodial proportions in both forelimb and hindlimb, and these are similar to other highly aquatic reptiles (plesiosaurs, ichthyosaurs, mosasaurs, and sea turtles) in sharp contrast to their more terrestrial relatives (Figs. 8 and 9B and figs. S24 to S26). This trend extends to aquatic mammals, which independently evolve enlarged autopodia despite having different body plans and locomotor modes (Fig. 4B and figs. S24 to S26).

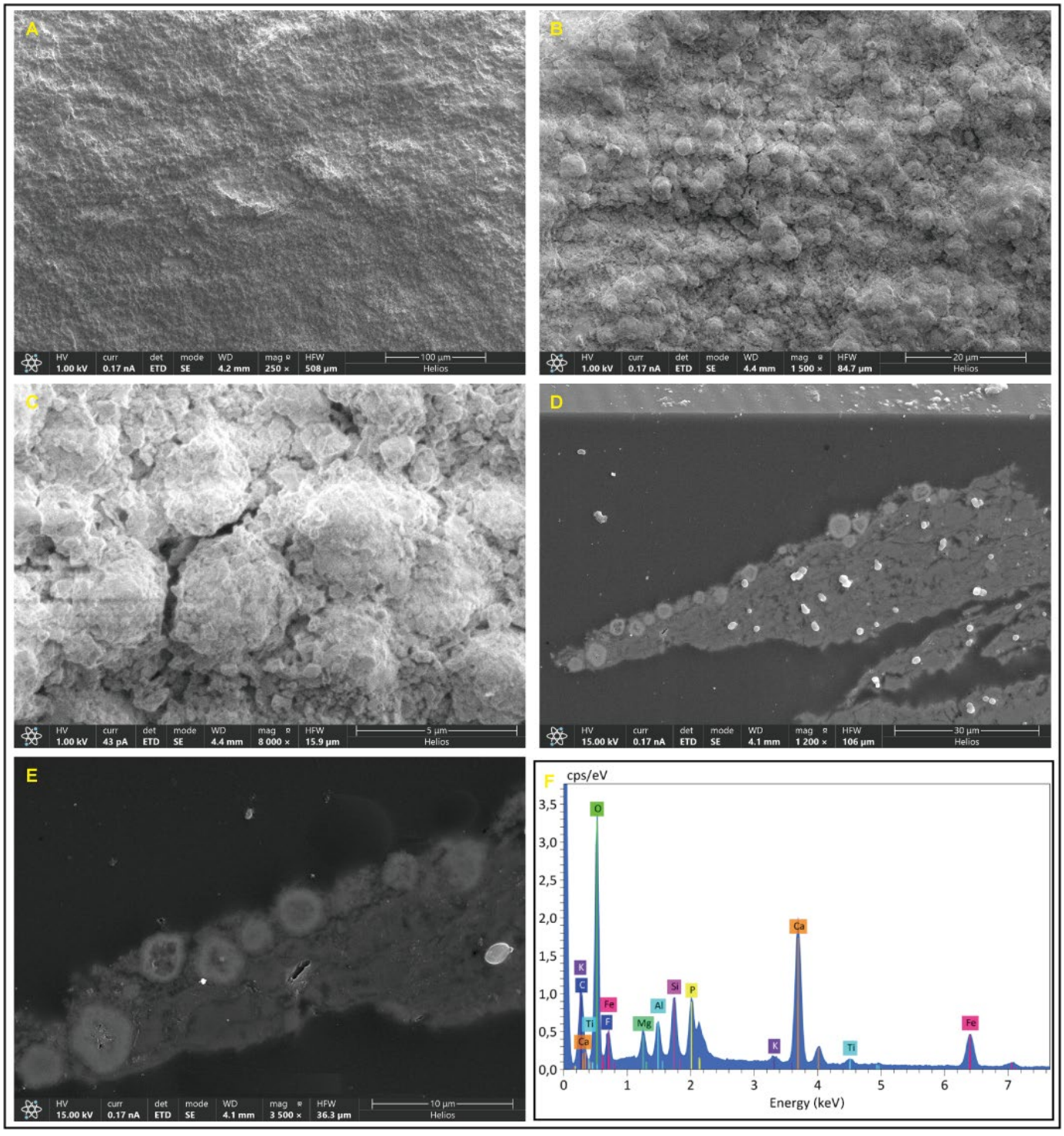

Fig. 5. Microstructure and element contents of sample 3 from the liver under SEM. This is sample 3 shown in fig. S9 located at the posterior part of the liver; (**A** to **C**) are the SEM images under different scales; (B) and (C) show the framboidal ferriferous mineral; (**D**) and (**E**) show the cross sections of the sample under different scales with the framboidal ferriferous mineral on the surface; (**F**) is the elemental analysis obtained from the region in (A).

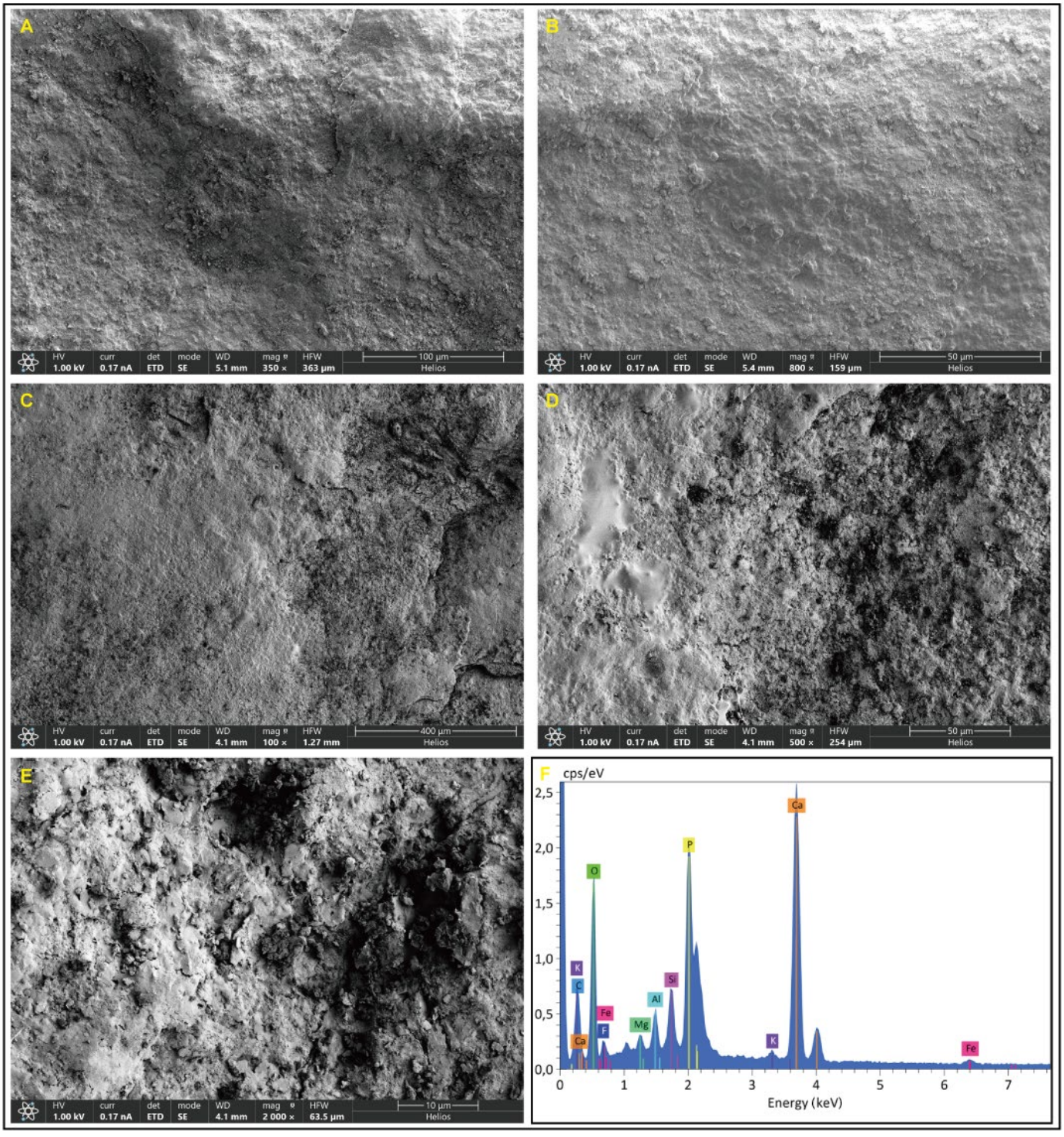

Fig. 6. Microstructure and element contents from the small intestine under SEM. This is sample 4 shown in fig. S9 located at the anterior part of the small intestine; (**A** to **E**) are the SEM images under different scales; (**F**) is the elemental analysis obtained from the region in (A).

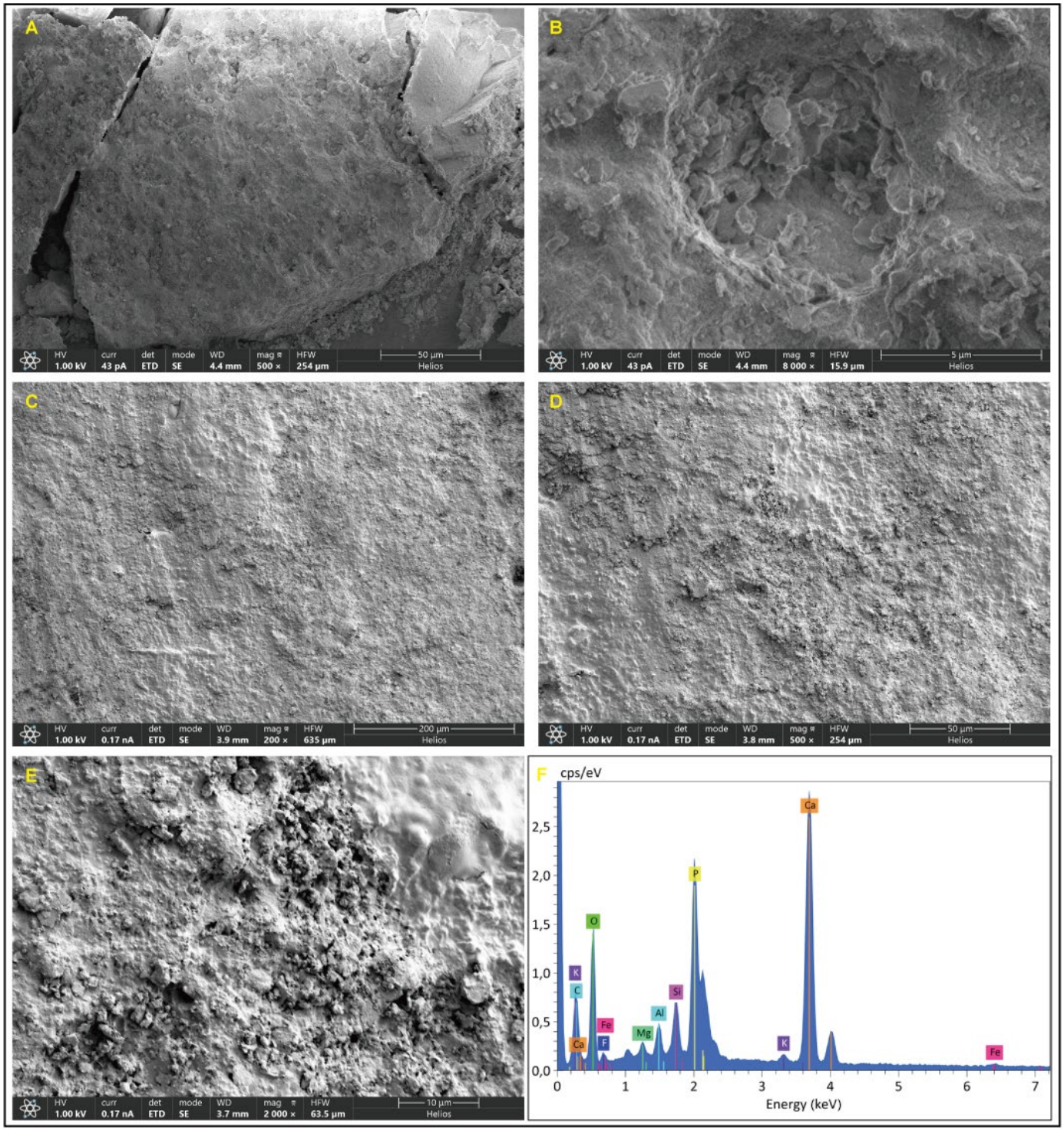

Fig. 7. Microstructure and element contents from the large intestine under SEM. This is sample 5 shown in fig. S9 located at the anterior part of the large intestine; (**A** to **E**) are the SEM images under different scales; (**F**) is the elemental analysis obtained from the region in (C).

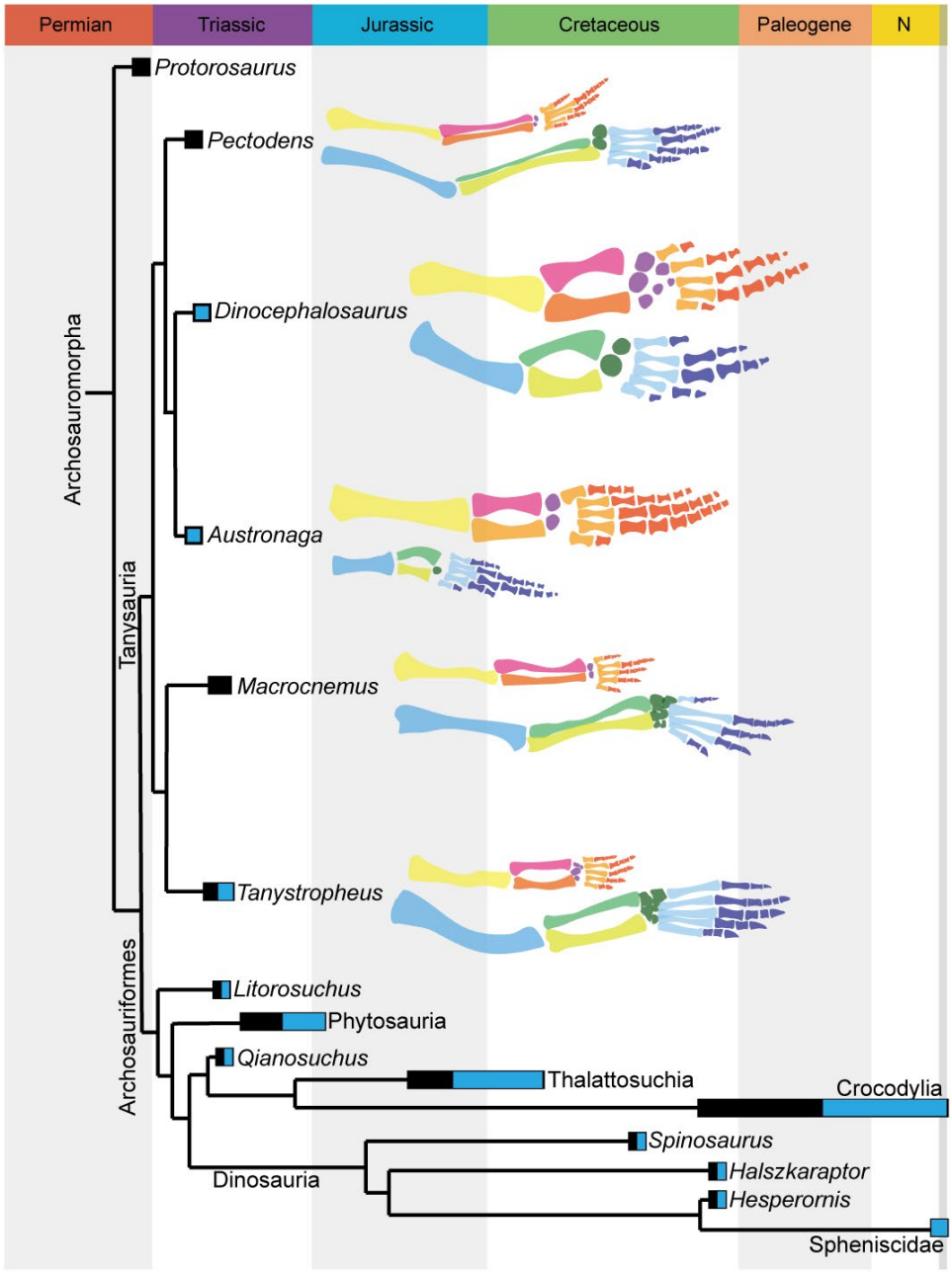

Fig. 8. Aquatic lineages in archosauromorphs with limb morphology in tanysaurs. Topology of tanysaurs is based on our phylogenetic result (fig. S20); subsection of crown group archosaurs is shown; terrestrial lineages in black, aquatic in blue, semiaquatic in half blue, and half black; homologous bony elements are of same colors in the forelimb (top) and hindlimb (bottom) near corresponding tanysaurian taxa.

Other characteristics reflecting an exclusively aquatic lifestyle, when compared to tanystropheids (*19*) and other stem archosaurs (*6*), include flattened long bones and phalanges; autopodial articulation facets undeveloped, thereby precluding flexion and extension; rudimentary joint morphology precluding effective limb-based locomotion on land; and rounded carpals and tarsals, much reduced in size and fewer in number (Fig. 8 and figs. S4 and S5). On the basis of the preserved limb posture (Fig. 1) and flattened joint surfaces, we infer that *Austronaga* at least partially used forelimb-generated thrust for aquatic propulsion (fig. S27). Unlike their terrestrial relatives (e.g., *Protorosaurus*, *Prolacerta*, *Pectodens*, *Macrocnemus*, and even the at least semiaquatic *Tanystropheus*) (*22*, *29*, *32*, *33*), where digits II and III are more gracile, *Austronaga* and *Dinocephalosaurus* evolved laterally broad and reinforced phalanges in preaxial digits I, II, and III (Fig. 8 and fig. S5), potentially forming hydrofoils for enhanced underwater lift generation (*47*). Both taxa display a complete loss of claws, with *Austronaga* additionally developing noteworthy hyperphalangy, a feature convergent with other highly aquatic amniotes that develop hydrodynamic flippers (*47*, *48*).

In contrast to the profound osteological modifications associated with aquatic adaptation, the gastrointestinal system of *Austronaga*

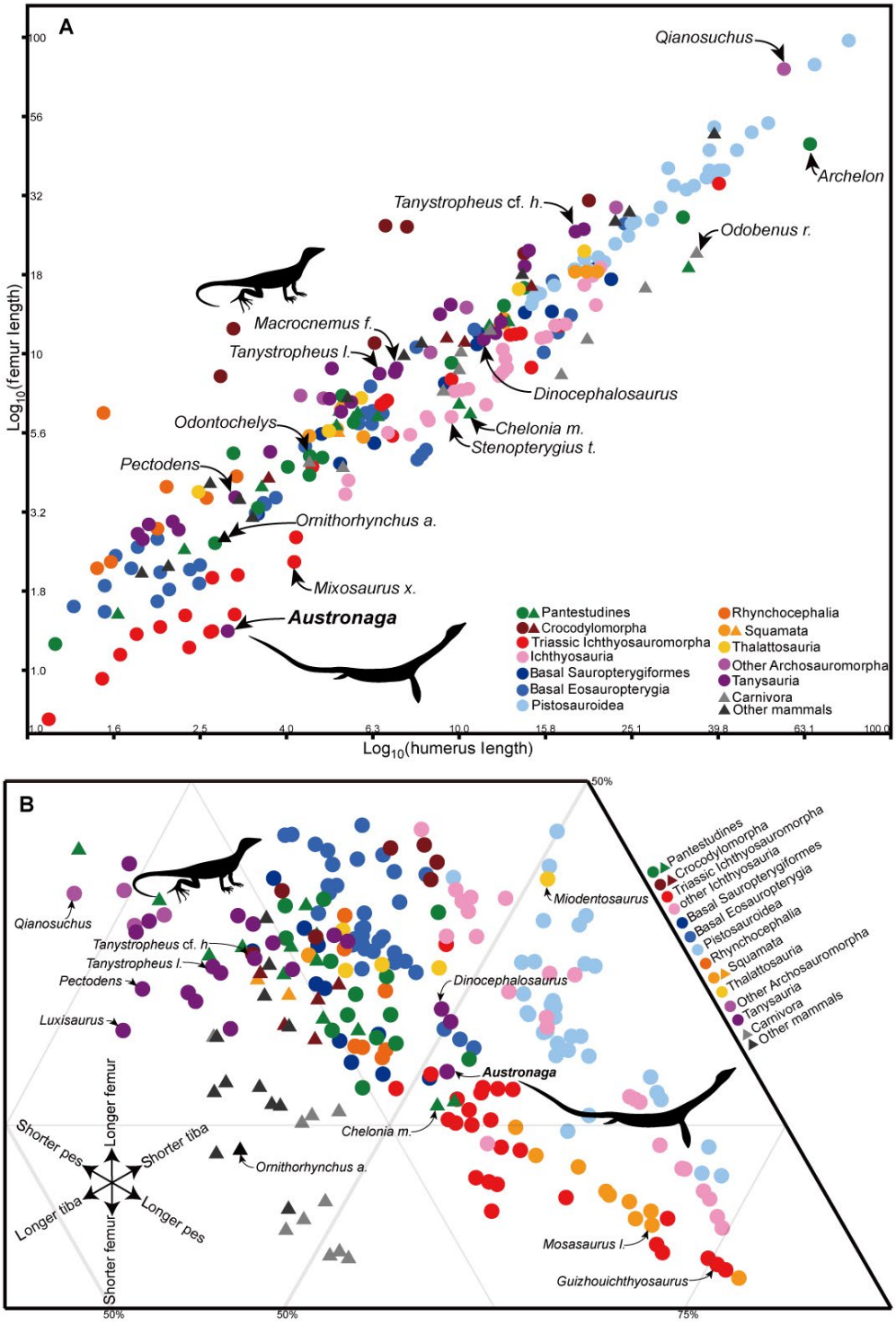

Fig. 9. Podial proportions in secondarily aquatic amniotes. (**A**) Ratio between long$_{10}$-transformed lengths of humerus and femur. (**B**) Ternary projection of lengths of femur, tibia, and pes. Two hundred and thirty taxa of both extant (triangle) and extinct (dot) secondarily aquatic amniotes are sampled, and *Austronaga* shows long humerus and large pes at an advanced stage of aquatic adaptation among other obligatorily marine amniotes.

exhibits minimal specialization (Fig. 3). In an exceptionally preserved Early Cretaceous theropod with internal soft tissues, the stomach failed to be preserved, purportedly because of the highly acidic environment caused by gastric secretions (*35*, *36*). This is not the case in IVPP V18579, where a clearly distinguishable stomach is preserved. The single-chambered large stomach of *Austronaga* contrasts with the derived two-chambered organization (sometimes with gastroliths) observed in crown archosaurs including birds and crocodylians (*49*), reflecting a morphologically plesiomorphic condition. The anterior part of the liver is likely overlain by the stomach, and we therefore assume that the liver was a larger organ than is exposed. The conspicuous color of the liver is assumed to be a derivative of hemoglobin, as shown by the enrichment of iron indicated by the scanning electron microscopy (SEM) analysis relative to the sediment (Fig. 6 and fig. S14). A relatively short, loosely coiled intestinal tract lacking colonic expansion in *Austronaga* is distinct from the elongated digestive systems of herbivorous reptiles like modern tortoise and iguana (*50*, *51*). This short intestine system indicates a rapid digestion, which is consistent with the piscivorous water monitor lizard (*51*). With 24 dorsal vertebrae, the torso of *Austronaga* is elongated compared to *Protorosaurus* and *Pectodens* (*20*, *22*), but the intestine does not show a corresponding elongation. This is in contrast to mustelid mammals but generally similar to the condition in snakes (*51*). The digestive tract of IVPP V18579 reflects a much lower selective pressure on the gastrointestinal morphology compared to the highly specialized body plan associated with its aquatic lifestyle.

Austronaga is unequivocally nested within Trachelosauridae and within Tanysauria more broadly. Its closest relative, *Dinocephalosaurus* (*25*), is also aquatic but displays less specialized aquatic modifications than *Austronaga* in its appendicular skeleton, whereas *Pectodens*, a member of the same family, exhibits a more terrestrial ecology (Fig. 8). The other tanysaur family, Tanystropheidae, also includes both predominantly terrestrial forms, such as *Macrocnemus*, and at least semi-aquatic forms, such as *Tanystropheus* (*24*), showing that a transition to marine habits occurred at least twice in tanysaur evolution. Therefore, compared to major marine reptilian lineages (e.g., sauropterygians, ichthyosaurs, and thalattosaurs), these tanysaurs represent the only group so far with known terrestrial early-diverging members and deeply nested aquatic taxa. This clade thus provides a unique opportunity to document the land-to-sea transition in reptile evolution during the Triassic.

The discovery of *Austronaga* reshapes our understanding of early archosauromorph ecology (fig. S27), demonstrating that marine colonization by stem archosaurs was earlier and more extensive than previously recognized (*8*, *44*). The land-to-sea transition occurred in this major reptilian clade at the beginning of the Mesozoic, similar to the more widely known and longer lasting marine reptile clades, such as Sauropterygia and Ichthyosauria, but also other exclusively Triassic clades like Thalattosauria (*2*, *3*). Collectively, these findings suggest a broader adaptive strategy among reptiles to survive in arid zones such as those in southern China during the Triassic (*1*).

MATERIALS AND METHODS

Fossil preparation and observation

The holotype of *Austronaga minuta* (IVPP V18579), consisting of two slabs, was needle-prepared by professional technicians at the IVPP, where the specimen is permanently housed. We examined the anatomy of this fossil through direct observation with the naked eye, a 10× magnifier, and optical microscopy. For computed laminography (CL), we used the 160-Micro-CL scanner at IVPP with a series of experiments with different parameter settings scanning all parts of the skeleton. Because of the low contrast between the bones and the limestone, as well as the thickness of the slabs, we only obtained informative results for the skull using a voltage of 110 kV, current of 50 mA, and achieving a voxel size of 35 μm (fig. S1). Photographic documentation of IVPP V18579 was performed under both visible and UV light using a digital mirrorless camera equipped with 50-mm prime and 100-mm macro lenses. UV photography was conducted in a darkroom with two 180-W UV-A lamps emitting a single wavelength of about 365 nm. Multiple resin and glass filters of yellow and orange colors were respectively used. The exposure times varied from 10 s to 1 min with different aperture values used in a series of tests. The images with optimal contrast were selected for figures (Figs. 2 and 3 and figs. S6 to S8). Under UV-induced fluorescence, the skeletal elements and particularly the visceral remains of this specimen exhibited enhanced color differentiation and contrast compared to visible-light observations.

We collected samples from representative marginal areas of the visceral remains in IVPP V18579, along with a rib distal end fragment and surrounding rock matrix for comparative microstructure and elemental analysis (fig. S9). Using needle preparation, we obtained sample fragments of no more than 1 mm^2, which were then mounted on stubs for SEM. SEM observation and imaging were performed using a Thermo Fisher Scientific Helios 5 CX DualBeam microscope at the IVPP, with gold sputter coating applied selectively based on sample conductivity. The parameters including voltage, current, detector, mode, magnification, and scale bar are provided in the images (Figs. 4 to 6 and figs. S10 to S14). Elemental analysis was conducted at 200× magnification across the entire field of view, with spectra acquired using Auto Slice View 4 software. For gold-coated samples, gold spectra were systematically excluded from the reported results.

Phylogenetic analysis

To assess the phylogenetic position of *Austronaga minuta* among tanysaurs, we updated the scoring of this taxon for the phylogenetic character-taxon matrix of Schoch *et al.* (see the Supplementary Materials for updated scorings) (*20*). This represents the most recent iteration of the matrix first introduced by Spiekman *et al.* (*19*) and subsequently modified by Wang *et al.* (*26*, *27*), Lu and Liu (*52*), and Spiekman *et al.* (*18*, *25*).

The dataset was analyzed in TNT 1.6 (*53*). Congruent with previous analyses of this matrix, *Czatkowiella harae*, *Tanystropheus* "*conspicuus*," and "*Tanystropheus antiquus*" were deactivated a priori, and characters 1, 2, 4, 5, 7, 9, 13, 35, 43, 62, 73, 77, 78, 83, 84, 88, 89, 110, 114, 118, 128, 136, 140, 144, 153, 158, 159, 162, 178, 185, 187, 194, 195, 200, 205, 209, 219, 220, 224, 230, 232, 242, 248, 251, 258, 259, 267, 276, 292, 294, 297, 298, 299, and 305 were treated as ordered. The analysis was conducted under equal weights for all the characters because the relative performance of implied weighting that penalizes homoplasy remains ambiguous in datasets containing fewer than 50 terminals (*54*). A traditional search was conducted with 1000 Wagner trees replications, random addition sequence, and tree bisection reconnection (TBR) for branch swapping holding 10 trees per replicate. Bremer and Bootstrap support (GC, groups recovered versus groups contradicted) values were calculated; the Bootstrap analysis using another Traditional search with 1000 iterations. Consistency and retention indices were calculated with the STATSb.run script in

TNT [see Spiekman *et al.* (*19*) for more details]. Because a large polytomy is formed by the resulting strict consensus tree (SCT) of the analysis, unstable terminal taxa were a posteriori omitted from the SCT to form a considerably better resolved reduced SCT using the iterPCR function in TNT (*55*).

Measurements and statistical analysis

We selected eight linear measurements on the limbs (lengths of humerus, femur, radius, tibia, manus, pes, forelimb, and hindlimb) of a broad sampling of secondarily aquatic tetrapods, excluding aquatic birds because of their highly modified forelimb morphology. Our first dataset of limbs measurements (data S1) is mainly derived from Motani and Vermeij (*43*) focusing on the lengths of humeri and femora, given that a longer humerus than femur is commonly present in marine tetrapods. The tetrapods with a highly aquatic lifestyle, which were categorized as the fourth and fifth marine adaptation steps, were used in this study. The second dataset of limb measurements (data S2) derives from Gutarra *et al.* (*56*), which was independent from that of Motani and Vermeij (*43*) with a broader investigation of the secondarily aquatic tetrapods. We selected the lengths of humerus, radius, manus, femur, tibia, and pes, as well as the lengths of forelimbs and hindlimbs with a combination of the Mesozoic reptile dataset and the extant aquatic tetrapod dataset in Gutarra *et al.* (*56*) except those of amphibians and penguins. We measured the eight podial lengths of tanysaurs, semiaquatic archosaurs, and early terrestrial archosauromorphs from direct recordings on the specimens or from scaled photographs using ImageJ and added them to the two datasets in this study with specimen numbers or references.

To compare the lengths between humerus and femur, and between forelimb and hindlimb, respectively, we plotted each pair of the two measurements in the coordinates without and with $\log_{10}$-transformation to reduce the body size influence. We used a ternary plot to visualize the proportions of stylopod, zeugopod, and autopod in the forelimb and hindlimb, respectively. The analyses were conducted in the paleontological statistics software package version 5.2.1 (*57*). The data, number, color, and symbol of each taxon were explained and displayed in the datasets and graphs (data S1 and S2, Fig. 9, and figs. S16 to S26).

Supplementary Materials

The PDF file includes:
Supplementary Text
Figs. S1 to S27
Legends for data S1 to S4

Other Supplementary Material for this manuscript includes the following:
Data S1 to S4

REFERENCES

1. M. J. Benton, The Triassic. *Curr. Biol.* **26**, R1214–R1218 (2016).
2. W. Wang, Q. Shang, L. Cheng, X. C. Wu, C. Li, Ancestral body plan and adaptive radiation of sauropterygian marine reptiles. *iScience* **25**, 105635 (2022).
3. R. Motani, D. Y. Jiang, G. B. Chen, A. Tintori, O. Rieppel, C. Ji, J. D. Huang, A basal ichthyosauriform with a short snout from the Lower Triassic of China. *Nature* **517**, 485–488 (2015).
4. B. P. Kear, V. S. Engelschion, O. Hammer, A. J. Roberts, J. H. Hurum, Earliest Triassic ichthyosaur fossils push back oceanic reptile origins. *Curr. Biol.* **33**, R178–R179 (2023).
5. S. J. Nesbitt, The early evolution of archosaurs: Relationships and the origin of major clades. *Bull. Am. Mus. Nat. Hist.* **352**, 1–292 (2011).
6. M. D. Ezcurra, The phylogenetic relationships of basal archosauromorphs, with an emphasis on the systematics of proterosuchian archosauriforms. *PeerJ* **4**, e1778 (2016).
7. M. D. Ezcurra, R. J. Butler, The rise of the ruling reptiles and ecosystem recovery from the Permo-Triassic mass extinction. *Proc. Biol. Sci.* **285**, 20180361 (2018).
8. A. E. Shipley, A. Elsler, S. A. Singh, T. L. Stubbs, M. J. Benton, Locomotion and the early Mesozoic success of Archosauromorpha. *R. Soc. Open Sci.* **11**, 231495 (2024).
9. A. Cau, V. Beyrand, D. F. A. E. Voeten, V. Fernandez, P. Tafforeau, K. Stein, R. Barsbold, K. Tsogtbaatar, P. J. Currie, P. Godefroit, Synchrotron scanning reveals amphibious ecomorphology in a new clade of bird-like dinosaurs. *Nature* **552**, 395–399 (2017).
10. N. Ibrahim, S. Maganuco, C. Dal Sasso, M. Fabbri, M. Auditore, G. Bindellini, D. M. Martill, S. Zouhri, D. A. Mattarelli, D. M. Unwin, J. Wiemann, D. Bonadonna, A. Amane, J. Jakubczak, U. Joger, G. V. Lauder, S. E. Pierce, Tail-propelled aquatic locomotion in a theropod dinosaur. *Nature* **581**, 67–70 (2020).
11. M. Fabbri, G. Navalón, R. B. Benson, D. Pol, J. O'Connor, B. A. S. Bhullar, G. M. Erickson, M. A. Norell, A. Orkney, M. C. Lamanna, S. Zouhri, J. Becker, A. Emke, C. Dal Sasso, G. Bindellini, S. Maganuco, M. Auditore, N. Ibrahim, Subaqueous foraging among carnivorous dinosaurs. *Nature* **603**, 852–857 (2022).
12. M. T. Stockdale, M. J. Benton, Environmental drivers of body size evolution in crocodile-line archosaurs. *Commun. Biol.* **4**, 38 (2021).
13. E. W. Wilberg, P. L. Godoy, E. F. Griffiths, A. H. Turner, R. B. J. Benson, A new early diverging thalattosuchian (Crocodylomorpha) from the Early Jurassic (Pliensbachian) of Dorset, U.K. and implications for the origin and evolution of the group. *J. Vertebr. Paleontol.* **42**, e2161909 (2022).
14. M. R. Stocker, L. J. Zhao, S. J. Nesbitt, X. C. Wu, C. Li, A short-snouted, Middle Triassic Phytosaur and its implications for the morphological evolution and biogeography of Phytosauria. *Sci. Rep.* **7**, 46028 (2017).
15. C. Li, X. C. Wu, Y. N. Cheng, T. Sato, L. Wang, An unusual archosaurian from the marine Triassic of China. *Naturwissenschaften* **93**, 200–206 (2006).
16. C. Li, X. C. Wu, L. J. Zhao, S. J. Nesbitt, M. R. Stocker, L. Wang, A new armored archosauriform (Diapsida: Archosauromorpha) from the marine Middle Triassic of China, with implications for the diverse life styles of archosauriforms prior to the diversification of Archosauria. *Naturwissenschaften* **103**, 95 (2016).
17. S. J. Nesbitt, M. R. Stocker, B. J. Small, A. Downs, The osteology and relationships of *Vancleavea campi* (Reptilia: Archosauriformes). *Zool. J. Linn. Soc.* **157**, 814–864 (2009).
18. S. N. Spiekman, M. D. Ezcurra, A. Rytel, W. Wang, E. Mujal, M. Buchwitz, R. R. Schoch, A redescription of *Trachelosaurus fischeri* from the Buntsandstein (Middle Triassic) of Bernburg, Germany: The first European *Dinocephalosaurus*-like marine reptile and its systematic implications for long-necked early archosauromorphs. *Swiss J. Palaeontol.* **143**, 10 (2024).
19. S. N. F. Spiekman, N. C. Fraser, T. M. Scheyer, A new phylogenetic hypothesis of Tanystropheidae (Diapsida, Archosauromorpha) and other "protorosaurs," and its implications for the early evolution of stem archosaurs. *PeerJ* **9**, e11143 (2021).
20. R. R. Schoch, H. D. Sues, G. Sobral, C. Kurz, A. Gottmann-Quesada, S. N. Spiekman, New data on the skull of *Protorosaurus speneri* (Reptilia: Archosauromorpha) and their phylogenetic significance. *J. Syst. Palaeontol.* **23**, 2496744 (2025).
21. O. Rieppel, The hind limb of *Macrocnemus bassanii* (Nopcsa) (Reptilia, Diapsida): Development and functional anatomy. *J. Vertebr. Paleontol.* **9**, 373–387 (1989).
22. C. Li, N. C. Fraser, O. Rieppel, L. Zhao, L. Wang, A new diapsid from the Middle Triassic of southern China. *J. Paleo.* **91**, 1306–1312 (2017).
23. C. Li, First record of protorosaurid reptile (Order Protorosauria) from the Middle Triassic of China. *Acta Geol. Sin.* **77**, 419–423 (2003).
24. S. N. Spiekman, J. M. Neenan, N. C. Fraser, V. Fernandez, O. Rieppel, S. Nosotti, T. M. Scheyer, Aquatic habits and niche partitioning in the extraordinarily long-necked Triassic reptile *Tanystropheus*. *Curr. Biol.* **30**, 3889–3895.e2 (2020).
25. S. N. F. Spiekman, W. Wang, L. Zhao, O. Rieppel, N. C. Fraser, C. Li, *Dinocephalosaurus orientalis* Li, 2003: A remarkable marine archosauromorph from the Middle Triassic of southwestern China. *Earth Environ. Sci. Trans. R. Soc. Edinb.* **114**, 218–250 (2023).
26. W. Wang, S. N. Spiekman, L. Zhao, O. Rieppel, T. M. Scheyer, N. C. Fraser, C. Li, A new long-necked archosauromorph from the Guanling Formation (Anisian, Middle Triassic) of southwestern China and its implications for neck evolution in tanystropheids. *Anat. Rec.* **308**, 2548–2562 (2023).
27. W. Wang, H. Lei, C. Li, A small-sized dinocephalosaurid archosauromorph from the Middle Triassic of Yunnan, southwestern China. *Vertebrata PalAsiatica* **62**, 13–32 (2024).
28. A. Rytel, C. Böhmer, S. N. F. Spiekman, M. Tałanda, Extreme neck elongation evolved despite strong developmental constraints in bizarre Triassic reptiles-implications for neck modularity in archosaurs. *R. Soc. Open Sci.* **11**, 240233 (2024).
29. S. Nosotti, *Tanystropheus longobardicus* (Reptilia, Protorosauria): Re-interpretations of the anatomy based on new specimens from the Middle Triassic of Besano (Lombardy, northern Italy). *Memorie della Societa Italiana di Scienze Naturali e del Museo Civico di Storia Naturale di Milano* **35**, 1–88 (2007).
30. N. C. Fraser, O. Rieppel, C. Li, A long-snouted protorosaur from the Middle Triassic of southern China. *J. Vertebr. Paleontol.* **33**, 1120–1126 (2013).
31. V. P. Jaquier, N. C. Fraser, H. Furrer, T. M. Scheyer, Osteology of a new specimen of *Macrocnemus* aff. *M. fuyuanensis* (Archosauromorpha, Protorosauria) from the Middle

Triassic of Europe: Potential implications for species recognition and paleogeography of tanystropheid protorosaurs. *Front. Earth Sci.* **5**, 91 (2017).
32. T. M. Scheyer, W. Wang, C. Li, F. Miedema, S. N. Spiekman, Osteological re-description of *Macrocnemus fuyuanensis* (Archosauromorpha, Tanystropheidae) from the Middle Triassic of China. *Vertebrata PalAsiatica* **58**, 169–187 (2020).
33. A. Gottmann-Quesada, P. M. Sander, A redescription of the early archosauromorph *Protorosaurus speneri* Meyer, 1832, and its phylogenetic relationships. *Palaeontographica Abteilung A Palaozoologie* **287**, 123–220 (2009).
34. O. Rieppel, C. Li, N. C. Fraser, The skeletal anatomy of the Triassic protorosaur *Dinocephalosaurus orientalis* Li, from the Middle Triassic of Guizhou Province, southern China. *J. Vertebr. Paleontol.* **28**, 95–110 (2008).
35. C. Dal Sasso, S. Maganuco, *Scipionyx samniticus* (Theropoda: Compsognathidae) from the Lower Cretaceous of Italy-Osteology, ontogenetic assessment, phylogeny, soft tissue anatomy, taphonomy and palaeobiology. *Memorie della Società Italiana di Scienze Naturali e del Museo Civico di Storia Naturale di Milano* 37. (2011): 1, pp. 1–3.
36. C. Dal Sasso, M. Signore, Exceptional soft-tissue preservation in a theropod dinosaur from Italy. *Nature* **392**, 383–387 (1998).
37. S. Renesto, M. Avanzini, Skin remains in a juvenile *Macrocnemus bassanii* Nopsca (Reptilia, Prolacertiformes) from the Middle Triassic of Northern Italy. *Neues Jahrbuch fur Geologie und Palaontologie-Abhandlungen* **224**, 31–48 (2002).
38. S. Renesto, A new specimen of *Tanystropheus* (Reptilia Protorosauria) from the Middle Triassic of Switzerland and the ecology of the genus. *Rivista Italiana di Paleontologia e Stratigrafia* **111**, 377–394 (2005).
39. M. J. Benton, Q. Zhang, S. Hu, Z. Q. Chen, W. Wen, J. Liu, J. Huang, C. Zhou, T. Xie, J. Tong, B. Choo, Exceptional vertebrate biotas from the Triassic of China, and the expansion of marine ecosystems after the Permo-Triassic mass extinction. *Earth Sci. Rev.* **125**, 199–243 (2013).
40. N. Ibrahim, P. C. Sereno, C. Dal Sasso, S. Maganuco, M. Fabbri, D. M. Martill, S. Zouhri, N. Myhrvold, D. A. Iurino, Semiaquatic adaptations in a giant predatory dinosaur. *Science* **345**, 1613–1616 (2014).
41. O. Rieppel, Feeding mechanics in Triassic stem-group sauropterygians: The anatomy of a successful invasion of Mesozoic seas. *Zool. J. Linn. Soc.* **135**, 33–63 (2002).
42. Y. Cheng, X. Wu, Q. Ji, Triassic marine reptiles gave birth to live young. *Nature* **432**, 383–386 (2004).
43. R. Motani, G. J. Vermeij, Ecophysiological steps of marine adaptation in extant and extinct non-avian tetrapods. *Biol. Rev. Camb. Philos. Soc.* **96**, 1769–1798 (2021).
44. C. M. Gordon, L. S. Freisem, C. T. Griffin, J. A. Gauthier, B.-A. S. Bhullar, Limb proportions predict aquatic habits and soft-tissue flippers in extinct amniotes. *Curr. Biol.* **35**, 5982–5998.e7 (2025).
45. P. D. Gingerich, Land-to-sea transition in early whales: Evolution of Eocene Archaeoceti (Cetacea) in relation to skeletal proportions and locomotion of living semiaquatic mammals. *Paleobiology* **29**, 429–454 (2003).
46. W. G. Joyce, J. A. Gauthier, Palaeoecology of triassic stem turtles sheds new light on turtle origins. *Proc. Biol. Sci.* **271**, 1–5 (2004).
47. A. Berta, *The Rise of Marine Mammals: 50 Million Years of Evolution* (JHU Press, 2017).
48. T. J. Fedak, B. K. Hall, Perspectives on hyperphalangy: Patterns and processes. *J. Anat.* **204**, 151–163 (2004).
49. K. V. Kardong, *Vertebrates: Comparative Anatomy, Function, Evolution* (McGraw-Hill, 2006).
50. B. Doneley, S. Simpson, A. M. Lennox, J. Chitty, Setting up and equipping a reptile practice. *Reptile Medicine and Surgery in Clinical Practice* , 115–124 (2017).
51. M. I. Hoppe, C. Meloro, M. S. Edwards, D. Codron, M. Clauss, M. J. Duque-Correa, Less need for differentiation? Intestinal length of reptiles as compared to mammals. *PLOS ONE* **16**, e0253182 (2021).
52. Y.-T. Lu, J. Liu, A new tanystropheid (Diapsida: Archosauromorpha) from the Middle Triassic of SW China and the biogeographical origin of Tanystropheidae. *J. Syst. Palaeontol.* **21**, 2250778 (2023).
53. P. A. Goloboff, S. A. Catalano, TNT version 1.5, including a full implementation of phylogenetic morphometrics. *Cladistics* **32**, 221–238 (2016).
54. M. D. Ezcurra, Exploring the effects of weighting against homoplasy in genealogies of palaeontological phylogenetic matrices. *Cladistics* **40**, 242–281 (2024).
55. D. Pol, I. H. Escapa, Unstable taxa in cladistic analysis: Identification and the assessment of relevant characters. *Cladistics* **25**, 515–527 (2009).
56. S. Gutarra, T. L. Stubbs, B. C. Moon, B. H. Heighton, M. J. Benton, The locomotor ecomorphology of Mesozoic marine reptiles. *Palaeontology* **66**, e12645 (2023).
57. Ø. Hammer, D. A. Harper, Past: Paleontological statistics software package for education and data analysis. *Palaeontol. Electronica* **4**, 1–9 (2001).

Acknowledgments: We acknowledge J. Ding for specimen preparation; W. Gao for photography; P. Yin for CL scan at the IVPP; J. Yang, J. Ma, and X. Jin from the Microscopy Laboratory, IVPP for SEM sampling and operation; Y. Pan and M. Clauss for preliminary discussion on soft tissue; G. Serafini for advice on UV photography; and G. Ugueto for the art reconstruction. The Willi Hennig Society and the program team of PAST are, respectively, acknowledged for making TNT and PAST publicly available. **Funding:** This research was supported by National Natural Science Foundation of China (42002019) and Youth Innovation Promotion Association of the Chinese Academy of Sciences. **Author contributions:** Conceptualization: W.W., C.L., N.C.F., S.N.F.S., and O.R. Investigation: W.W., N.C.F., S.N.F.S., Z.L., and T.M.S. Methodology: W.W., S.N.F.S., N.C.F., and Z.L. Resources: C.L., W.W., and H.L. Funding acquisition: C.L. and W.W. Data curation: C.L., W.W., Z.L., and S.N.F.S. Validation: W.W., S.N.F.S., N.C.F., and Z.L. Formal analysis: S.N.F.S. and W.W. Software: W.W. Visualization: W.W., S.N.F.S., Z.L., and N.C.F. Supervision: C.L., N.C.F., and T.M.S. Writing—original draft: W.W., N.C.F., S.N.F.S., and Z.L. Writing—review and editing: C.L., N.C.F., T.M.S., Z.L., O.R., S.N.F.S., and H.L. Project administration: C.L. and W.W. **Competing interests:** The authors declare that they have no competing interests. **Data, code, and materials availability:** All data and code needed to evaluate and reproduce the results in the paper are present in the paper and/or the Supplementary Materials. This study did not generate new materials.

Submitted 25 August 2025
Accepted 25 June 2026
Published 29 July 2026
10.1126/sciadv.aeb7528

Highly aquatic marine stem archosaur with soft tissue preservation

Wei Wang, Nicholas C. Fraser, Stephan N. F. Spiekman, Zhiheng Li, Olivier Rieppel, Hong Lei, Torsten M. Scheyer, and Chun Li

Sci. Adv. **12** (31), eaeb7528. DOI: 10.1126/sciadv.aeb7528